# Graphene-Modified Electrode for the Selective Determination of Uric Acid Under Coexistence of Dopamine and Ascorbic Acid

*Mingyong Chao*[*], *Xinying Ma  and Xia Li*

Department of Chemistry and Chemical Engineering, Heze University, Heze 274015, PR China.
[*]E-mail: chao@rychem.com

A graphene-modified electrode for selective determination of uric acid was prepared. The electrochemical behaviours of uric acid at the graphene-modified electrode was investigated by cyclic voltammetry and the results showed that the graphene film on electrode exhibited excellent electrocatalytic activity for the electrochemical oxidation of uric acid in phosphate buffer solution (pH 4.0). Using the graphene-modified electrode, uric acid under coexistence of dopamine and ascorbic acid was successfully determined with good peak separation. The values of linearity range, correlation coefficient and limit of detection for uric acid were $2.00\times10^{-6}$ to $1.20\times10^{-4}$ mol/L, 0.9975 and $6.00\times10^{-7}$ mol/L respectively. The graphene-modified electrode is of excellent sensitivity, selectivity and stability, and has been successfully used for determination of uric acid in human urine.

## 1. INTRODUCTION

Uric acid (UA), a very important biological molecule present in body fluids, indicates symptoms of several diseases such as pneumonia, fatal poisoning, and toxaemia of pregnancy when its level goes extremely abnormal [1], which makes determination of UA concentration in urine very important. Various methods have been developed for determination of UA, such as spectrometry [2, 3], liquid chromatography [4], and electrochemical methods using ion-exchange membrane coated electrode [5, 6], chemically modified electrode [7-10] or enzyme-modified electrode [11-13], but due to the great clinical significance of UA determination, many researchers are still striving for better methods. UA is an electroactive molecule that can be irreversibly oxidized into allantoin in aqueous solution [11], it usually coexists with dopamine (DA) and ascorbic acid (AA) in body fluids. Because

these molecules have close oxidation potentials at bare electrode, determination of UA in body fluids using bare electrode becomes rather difficult.

Graphene is an allotrope of carbon, whose structure is one-atom-thick planar sheets of $sp^2$-bonded carbon atoms that are densely packed in a honeycomb crystal lattice [14]. Graphene possesses outstanding characteristics such as having a large specific surface area, excellent conductivity, and strong mechanical strength. It has been used to prepare a new generation of electrodes for electrochemical studies [15-19].

In this paper, a convenient and highly selective graphene-modified glassy carbon electrode (GME) is described. Using the GME, an electrochemical sensor was fabricated and its electrochemical properties were investigated. Selective determination of UA by this sensor in the presence of high concentrations of DA and AA was demonstrated. It was found that the modified electrode not only exhibited strong electrocatalytic activity for oxidation of UA, DA and AA, but also resolved their voltammetric responses into three well-defined peaks. This sensor showed excellent sensitivity and selectivity in determination of UA in human urine. Compared with reported electrochemical methods for determination of DA, this method gives much wider linearity range, providing greater convenience in sample analysis because the UA concentrations in biological samples are normally not known.


## 2. EXPERIMENTAL

### 2.1 Reagents and solutions

Graphite powder (<20 μm) was obtained from Qindao Graphite Corporation (Qingdao, China). Sodium borohydride was obtained from Tianjin Daofu Chemical New Technique Development Co., Ltd. (China). Dopamine (DA) was purchased from the National Institute for the Control of Pharmaceutical and Biological Products (Beijing, China). Ascorbic acid (AA) and uric acid (UA) were purchased from Beijing Chemical Factory (China). The $4.0 \times 10^{-3}$ mol/L UA standard solution was prepared by dissolving uric acid in 0.1 mol/L sodium carbonate. All other reagents used in this study were of AR grade purchased from Beijing Chemical Reagent Company (Beijing China). The phosphate buffer solution (PBS) (pH 4.0) was prepared by mixing 0.2 mol/L disodium hydrogen phosphate and 0.1 mol/L citric acid. All aqueous solutions were prepared using double distilled water.


### 2.2 Apparatus

Electrochemical measurements was conducted on a CHI 660C Electrochemical Workstation (Chen-hua, Shanghai, China). Infrared spectra were recorded using a Varian 660-IR spectrometer (Agilent, America). Raman spectra was obtained using a LabRAM-HR Raman Spectrometer (Jobin-Yvon, France). Scanning electron microscope (SEM) image was obtained using a field emission SEM Sirion 200 (FEI, America). TEM image was obtained using a JEM-2010 transmission electron

microscope (JEOL, Japan). All electro-chemical experiments were carried out using a three-electrode system consisted of a working electrode (a bare or graphene-modified glassy carbon electrode, 3 mm in diameter) a counter electrode (a platinum wire electrode), and a reference electrode (a Ag/AgCl electrode). Acidity was measured by a PHS-3B Precision pH Meter (Shanghai, China), and all sonication was done using a KQ-100 Ultrasonic Cleaner (Kunshan, China).

*2.3 Preparation of the Nano-graphene and Graphene Modified Electrode*

Nano-graphene power was prepared according to a literature reported procedure. Briefly, Graphite powder was oxidized with potassium permanganate in sulfuric acid to give graphite oxide, which was then dispersed in water by sonication to give a colloidal solution. Reduction with sodium borohydride and washing work-up gave a Nano-graphene power [20-23]. Then a graphene-modified electrode was prepared as follows, 5 mg of the nano-graphene powder was dispersed in 10mL of double distilled water with ultrasonication for 20min to give a black graphene suspension. A bare glassy carbon electrode (GCE, 3.8 mm in diameter) was polished with abrasive paper (grit 2000) and wet alumina powder (0.05µm) before it was used, rinsed ultrasonically with 1:1 HNO3, absolute ethanol, and distilled water, respectively, and dried under infrared lamp. Then 4 µL of the graphene suspension was cast on the surface of GCE and dried under infrared lamp to give a graphene-modified electrode.

*2.4 Electrochemical measurement*

Using a GME as working electrode, a Ag/AgCl electrode as reference electrode and a platinum as counter electrode, cyclic voltammetry was used in the electrochemical measurements with a scan rate of 120 mV/s. Cyclic voltammograms (CVs) were obtained by immersing the GME in UA standard solution buffered by phosphates and scanning in the potential range from 0.2 V to 0.9 V. Upon completion of each scan, the modified electrode was placed in a blank buffer solution and cyclic scan was continued until no peak comes out, then the electrode was washed with water and dried with filter paper for reuse.

## 3. RESULTS AND DISCUSSION

*3.1 Characterization of graphite/graphene/GME*

Figure 1 shows the IR spectra of graphite and graphene. Table 1 shows the functional groups of graphene and their corresponding wave numbers. Figure 1 and Table 1 demonstrate that graphene has been successfully prepared and contains C–O–C and C–OH functional groups. These functional groups

as well as defects in graphene can improve the water solubility of graphene, making its dispersion in water more stable.
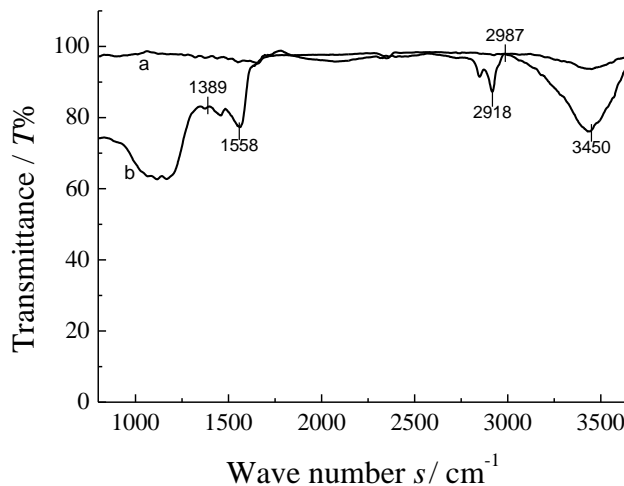


**Figure 1.** IR spectra of (a) graphite and (b) graphene

**Table 1.** Functional groups of graphene and their corresponding wave numbers

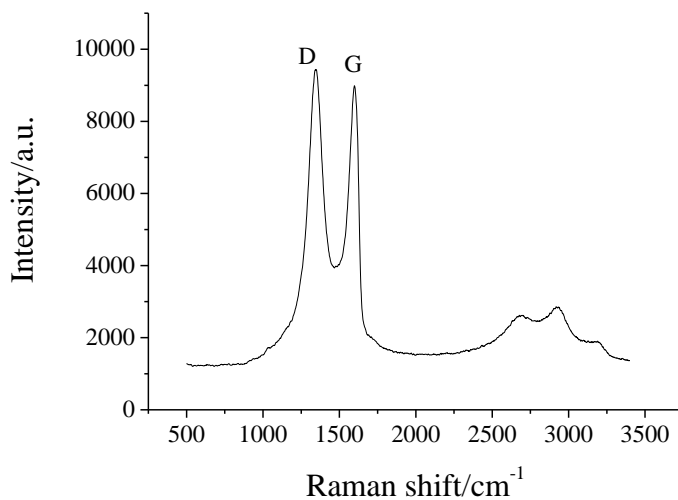| Functional group | Wave number $\sigma$ /cm$^{-1}$ |
|:---:|:---:|
| -OH | 3450 |
| C=C | 1558 |
| phenyl | 2800-3000 |
| C-O-C | 1110-1200 |



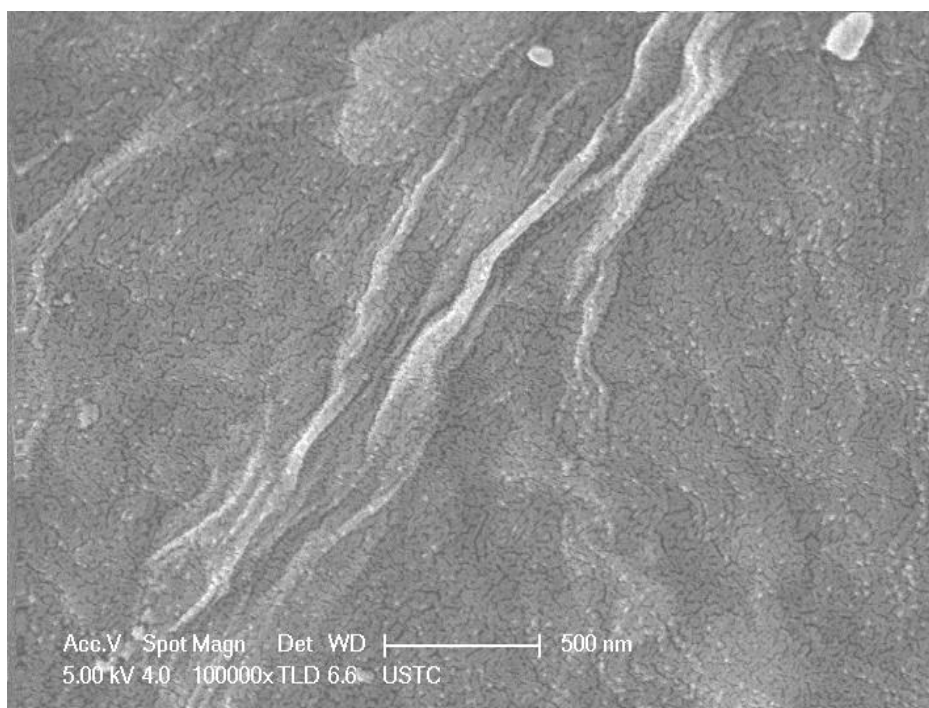**Figure 2.** Raman spectra of graphene

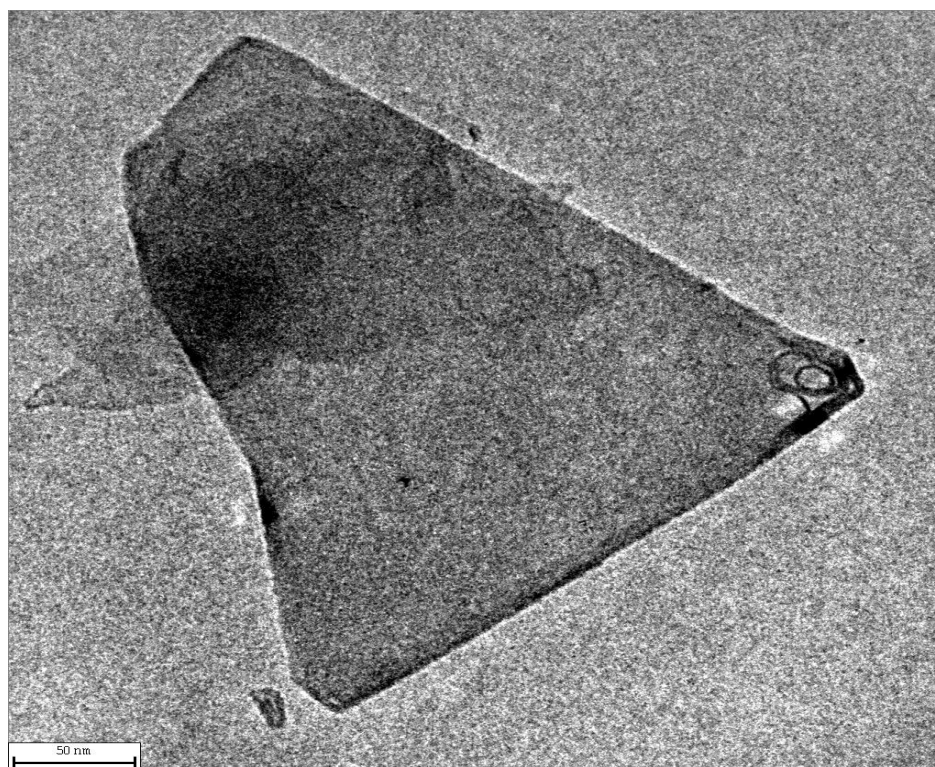**Figure 3.** SEM image of graphene-film modified GCE



**Figure 4.** TEM image of graphene

Figure 2 shows the Raman spectrum of graphene, which shows the D band at 1347 cm$^{-1}$ that arose from sp$^3$-hybridized carbon as well as the G band at 1597 cm$^{-1}$ that shows in-phase vibration of the graphite lattice. The relative intensity ratio of the D and G lines provides a sensitive measure of the disorder and crystallite size of the graphitic layers. Figure 3 shows the SEM image of the graphene film on the GCE, revealing the crumple and wrinkle structure of the graphene film. Figure 4 shows the TEM image of graphene nanosheets, revealing its mono- or few-layer planar sheet-like morphology.

## 3.2 Optimization of GME

Oxidation peak currents are greatly influenced by the amount of graphene deposited on glassy carbon electrode. When 4 μL of graphene suspension of different concentration are deposited on the surface of GCE, experiments show that greater graphene concentration gives higher UA oxidation peak current at the modified electrode. The oxidation peak current of UA reach maximum when the concentration of graphene is 0.5 mg/mL. Concentration of graphene greater than 0.5 mg/mL causes the graphene coating on electrode surface excessively thick. Due to the excessive thickness of graphene coating, the catalyst can not be employed efficiently and the diffusion of catalytic substrate to electrode surface becomes more difficult, thus the oxidation peak current is reduced. In our experiments, 4 μL of graphene suspension with a concentration of 0.5 mg/mL was used in the preparation of graphene-modified electrode.

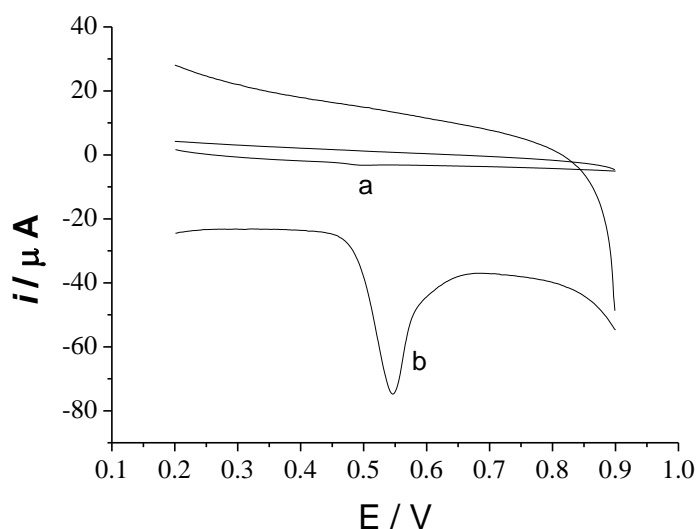## 3.3 Electrochemical behaviour of uric acid at bare and graphene-modified electrode



**Figure 5** Cyclic voltammograms of  6.0×10$^{-5}$ mol/L UA at the bare electrode (a) and the graphene-modified  electrode (b) in pH 4.0 PBS, scan  rate:120mV/s.

Cyclic voltammograms of UA at the bare electrode and the graphene modified electrode are shown in Figure 5, which shows that the current response of UA at the bare electrode is weak, $E_{pa}$ = 0.50V, $i_{pa}$ = -0.52µA and the current response of UA at the modified electrode is much better, $E_{pa}$ = 0.54V, $E_{pa}$ = -51.55µA.

Oxidation peak current of UA at the modified electrode is almost 100 times of the current response at the bare electrode, which indicates that graphene film can significantly catalyze the UA oxidation process and the electron transfer rate of UA in graphene film is much faster.
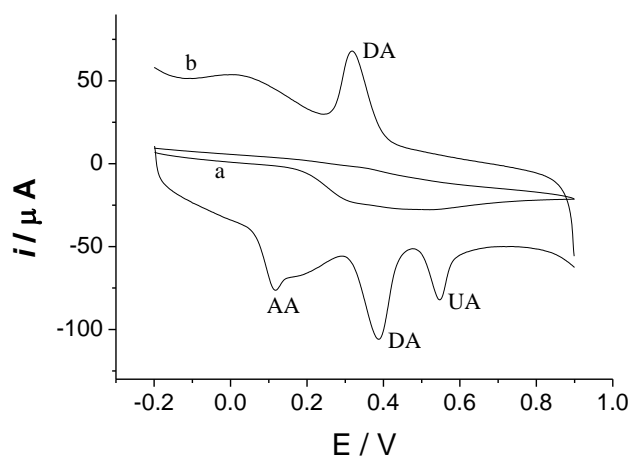


**Figure 6.** Cyclic voltammograms of $1.0 \times 10^{-5}$ mol/L uric acid , $1.0 \times 10^{-4}$ mol/L dopamine  and $1.0 \times 10^{-3}$ mol/L ascorbic acid  at the bare electrode (1) and the graphene modified (2)  in pH 4.0 PBS.
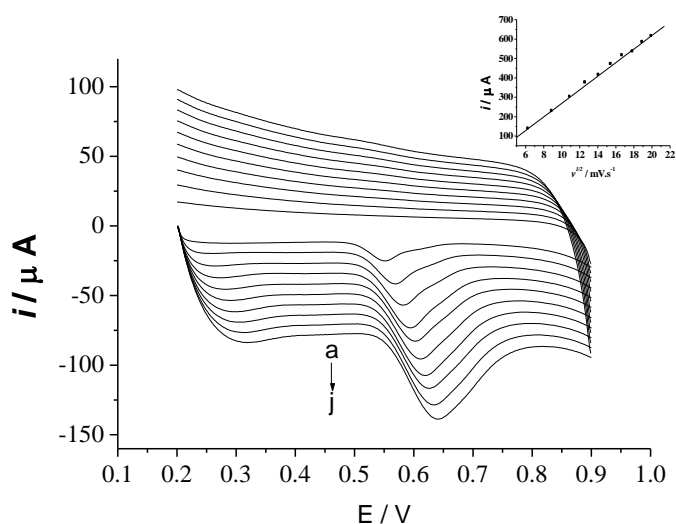


**Figure 7.** Cyclic voltammograms of $5.0 \times 10^{-6}$ mol/L UA at the graphene-modified electrode. Each of the letters from a to j correspond to scan rates of 40, 80, 120, 160, 200, 240, 280, 320, 360 and 400, respectively (in mV/s). Inset is the plot of the oxidation peak current of UA versus scan rates.

This may be attributed to the special nano-mesh structure of graphene, which has a large specific surface area and a large number of defects.

These defects are resulted from the redox preparation process and serve as highly active reaction sites, making the UA activity at the modified electrode significantly improved and the response signal greatly increased. From the CVs of UA at the modified electrode, we can see that there is no reduction peak of UA, only its oxidation peak is observed, which demonstrates that the reaction is irreversible.In a pH 4.0 phosphate buffer solution, UA, AA (100) and DA (10) are shown as one broad oxidation peak at the bare electrode as shown in Figure 6(a), while at the graphene modified electrode, their oxidation peaks were effectively separated as shown in Figure 6(b), the oxidation peak potentials of AA, DA and UA are 0.11V, 0.38V and 0.54V respectively. The separation of peak potentials is 0.43V and 0.16V for AA-UA and DA-UA respectively, which is large enough to determin UA individually. This demonstrates that UA can be successfully determined in presence of dopamine and ascorbic acid when using the modified electrode. While in some reported literatures for selective determination of UA [9, 24, 6], the interference of DA was not discussed.

Figure 7 gives the cyclic voltammetry curves of UA at different scan rates, which shows that the oxidation peak potential shift positively with scan rate increasing, and the oxidation peak current is proportional to the square root of scan rates when scan rates are between 40 and 400mV/s. The linear equation is $i_{pa}$ (A) = $-7.99 \times 10^{-6}$ $-3.50 \times 10^{-6} v^{1/2}$ (mV/s), r = 0.9989. This shows that the electrode reaction is controlled by the diffusion process, which is the typical characteristics of irreversible reactions. Kumar et al. reported the same electrode process of UA at polymerized luminol film modified electrode [25]. Possible oxidation mechanism of UA at electrode is shown in Scheme 1.

Main product of the electrochemical oxidation is 4,5-dihydroxyluric acid, which is unstable and mostly decomposes into allantoin. This explains why the cathodic peak is not obvious in cyclic voltammogram [26].
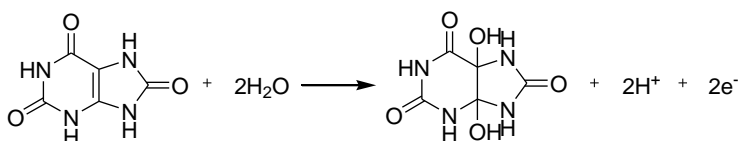


**Scheme 1.** Electrochemical oxidation mechanism of UA.

*3.4 Optimization of Conditions for the determination of UA*

*3.4.1 Effect of Solution pH*

The effect of solution pH on the electrochemical signal was analyzed in PBS. Figure 8 shows the influence of solution pH on UA oxidation peak potential and peak current. Using phosphate buffer

solution of various pH, results show that with pH increasing, UA oxidation peak shifts negatively, which indicates that the UA oxidation reaction involves the protons, UA oxidation peak potential changes linearly depending on a pH from 2.2 to 8.0, and the equation is $E_{pa} = 0.91 - 0.079pH$, r = 0.9996. In a pH from 2.2 to 8.0 and a potential from 0.2 to 0.9, oxidation peak current firstly increases with increasing pH and reaches maximum at pH 4.0, then decreases as pH continues to increase, which also indicates that the UA oxidation reaction involves the protons. Therefore, a pH 4.0 buffer solution was chosen. In reported literatures, maximum electric currents of UA at nafion-coated carbon paste electrode [6] and PtAu hybrid film modified electrode [27] were also obtained at pH 4.0.
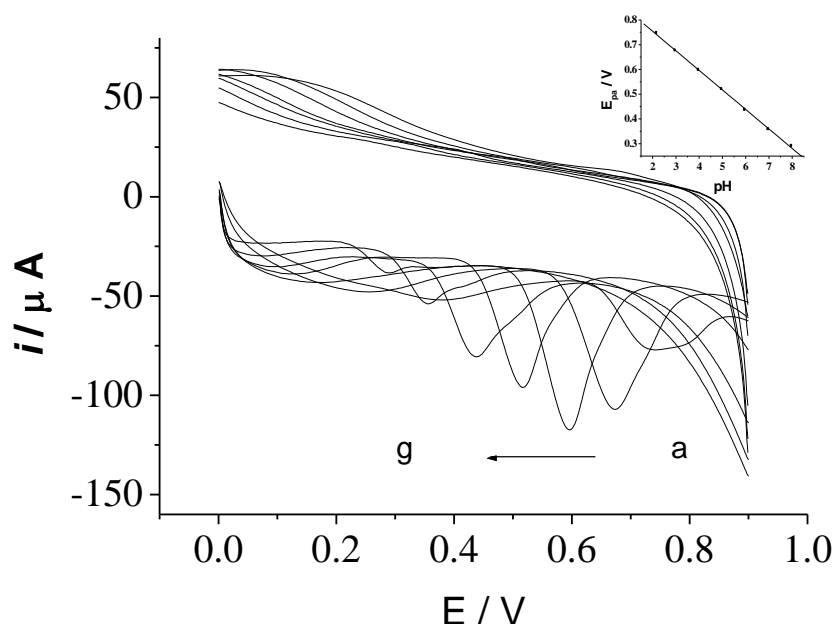


**Figure 8.** Cyclic voltammograms of $4.0 \times 10^{-5}$ mol/L UA at different pH. Each of the letters from a to g correspond to pH of 2.2, 3.0, 4.0, 5.0, 6.0, 7.0 and 8.0, respectively. Inset is the plot of the peak potential of UA versus pH value of buffer solutions.

*3.4.2 Effect of Stirring Time*

Stirring time exerts great influence on UA oxidation peak current at the modified electrode. Measurements were made with various stirring time at a UA concentration of $2.0 \times 10^{-5}$ mol/L. Results showed that additional stirring could improve the sensitivity of the method, the oxidation peak current increased with increasing stirring time and reached maximum at 120 s. This is because excess potential caused by concentration difference of UA on electrode surface becomes smaller with better mixing, resulting increased response current. Hence, a stirring time of 120 s was chosen in this study.

*3.5 Linearity range and detection limit*

In pH 4.0 phosphate buffer solution, The oxidation peak current of UA at the graphene-modified electrode is linearly proportional to its concentration in a range from $2.00\times10^{-6}$ to $1.20\times10^{-4}$ mol/L (Figure 9), with a correlation coefficient of 0.9975 and a detection limit of $6.00\times10^{-7}$ mol/L. The linear regression equation is $i_{Pa}$ (A) $= 5.64\times10^{-6} + 1.98C$.
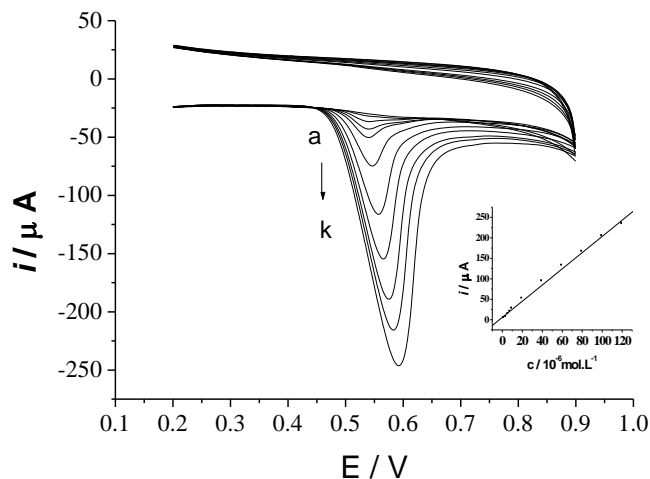


**Figure 9.** Cyclic voltammograms of UA at GME at different concentration. Each of the letters from a a to k correspond to concentrations of $2.00\times10^{-6}$ , $4.00\times10^{-6}$, $6.00\times10^{-6}$, $8.00\times10^{-6}$, $1.00\times10^{-5}$, $2.00\times10^{-5}$, $4.00\times10^{-5}$, $6.00\times10^{-5}$, $8.00\times10^{-5}$, $1.00\times10^{-4}$ and $1.20\times10^{-4}$, respectively (in mol/L). Inset is the plot of the oxidation peak current versus concentration of UA.

**Table 2.** Comparison of this work and literature reported ones

| Electrode | Modifier used | pH | Detection limit (M) | Linearity range(M) | Ref |
|---|---|---|---|---|---|
| glassy carbon | polymerized luminol | 7.0 | $2.0\times10^{-6}$ | $3.0\times10^{-5}$ - $1.0\times10^{-3}$ | [25] |
| carbon paste | palladium nanoparticle-loaded carbon nanofibers | 4.5 | $7.0\times10^{-7}$ | $2.0\times10^{-6}$ - $2.0\times10^{-4}$ | [28] |
| glassy carbon | hollow nitrogen-doped carbon microspheres | 7.0 | $4.0\times10^{-8}$ | $5.0\times10^{-6}$ - $3.0\times10^{-5}$ | [29] |
| graphite | functionalized-graphene | 7.0 | $4.5\times10^{-7}$ | $1.75\times10^{-6}$ - $9.0\times10^{-5}$ | [30] |
| phosphorylated zirconia-silica composite electrode | methylene blue | 7.4 | $3.7\times10^{-6}$ | $2.2\times10^{-5}$ - $3.5\times10^{-4}$ | [31] |
| glassy carbon | PtAu hybrid film | 4.0 | - | $2.1\times10^{-5}$ - $3.3\times10^{-4}$ | [27] |
| glassy carbon | helical carbon nanotubes | 6.8 | $1.5\times10^{-6}$ | $6.7\times10^{-6}$ - $6.5\times10^{-5}$ | [32] |
| glassy carbon | evans blue | 4.5 | $2.0\times10^{-6}$ | $3.0\times10^{-5}$ - $1.1\times10^{-4}$ | [33] |
| pyrolytic graphite | dopamine | 6.5 | $1.4\times10^{-6}$ | $2.5\times10^{-6}$ - $3.0\times10^{-5}$ | [34] |
| glassy carbon | vinyl alcohol | 7.0 | $6.0\times10^{-7}$ | $2.0\times10^{-6}$ - $5.0\times10^{-5}$ | [35] |
| glassy carbon | 2-amino-1,3,4-thiadiazole | 5.0 | $1.9\times10^{-7}$ | $1.0\times10^{-5}$ - $1.0\times10^{-4}$ | [36] |
| glassy carbon | graphene | 4.0 | $6.0\times10^{-7}$ | $2.0\times10^{-6}$ - $1.2\times10^{-4}$ | this work |

To evaluate our research results, the linearity range and detection limit in this work are compared with literature reported ones in table 2. These data show that the detection limit is comparable or better in most cases than the reported ones for electrochemical determination of UA at the surface of different modified electrodes. The linearity range in this work is much better than most reported ones, which provides convenience in analysis because the concentrations of biological samples are normally not known.

## 3.6 Interference Studies

Potential interference to UA response signal from common substances contained in urine was investigated in pH 4.0 phosphate buffer solution under optimized conditions. When the relative error is less than ±5%, no interferences were observed in the presence of glucose (1000), sucrose (1000), citrate (1000), urea (500), $K^+$ (500), $Na^+$ (500), $Mg^{2+}$ (200) and $Zn^{2+}$ (200).

## 4. ANALYTICAL APPLICATION

Fresh urine sample (25.00 mL) was added to a 100mL volumetric flask, followed by the addition of $Na_2CO_3$ solution (2.00 mL), then the solution in the flask was diluted to mark with double distilled water. A certain amount of the above prepared solution was taken and diluted with pH 4.0 PBS, and then measurement was made in accordance with the electrochemical measurement procedure. Recoveries were calculated with oxidation peak current value and results are shown in Table 3.

**Table 3.** Determination results of NE in injection (n=6)

| Sample | Content($\times 10^{-6}$mol/L) | R.S.D(%) | Added($\times 10^{-6}$mol/L) | Found($\times 10^{-6}$mol/L) | Recovery(%) |
|--------|--------|--------|--------|--------|--------|
| 1 | 3.75 | 3.3 | 4.00 | 7.81 | 101.5 |
| 2 | 4.39 | 2.1 | 4.00 | 8.33 | 98.5 |
| 3 | 4.34 | 2.9 | 4.00 | 8.18 | 96.0 |

## 5. CONCLUSION

A graphene-modified electrode for selective detection of uric acid was prepared. In comparison with the bare electrode, the graphene-modified electrode exhibited excellent electro-catalytic activity towards UA electrochemical oxidation, which may be attributed to the large specific surface area of graphene and the large number of defects in graphene. These defects serve as highly active sites for reaction, making UA reaction at the graphene-modified electrode significantly improved and electrochemical response signal greatly increased; The oxidation peak current of UA at the graphene-modified is linearly proportional to its concentration in a range from $2.00\times 10^{-6}$ to $1.20\times 10^{-4}$ mol/L; The

graphene-modified electrode is of excellent sensitivity, selectivity and stability. Using the graphene-modified electrode, UA was determined in the presence of dopamine and ascorbic acid with good peak seperation. The newly established method for determination of UA has been successfully used in human urine analysis.

**References**

1. V. V. S. E. Dutt and H. A. Mottola, *Anal Chem*, 46 (1974) 1777
2. M. H. Abdel-hay, M. H. Barary, M. A. Elsayed and E. M. Hassan, *Anal Lett*, 24 (1991) 1517
3. T. M. C. C. Filisetti-Cozzi and N. C. Carpita, *Anal Biochem*, 197 (1991) 157
4. S. P. Ferraris, H. Lew and N. M. Elsayed, *Anal Biochem*, 195 (1991) 116
5. J.-M. Zen, *Analyst*, 123 (1998) 1345
6. J.-M. Zen and C.-T. Hsu, *Talanta*, 46 (1998) 1363
7. Z. Gao and H. Huang, *Chem Commun*, (1998) 2107
8. Z. Gao, K. S. Siow, A. Ng and Y. Zhang, *Anal Chim Acta*, 343 (1997) 49
9. K. Shi and K.-K. Shiu, *Electroanalysis*, 13 (2001) 1319
10. J.-M. Zen, Y.-J. Chen, C.-T. Hsu and Y.-S. Ting, *Electroanalysis*, 9 (1997) 1009
11. E. Gonzalez, F. Pariente, E. Lorenzo and L. Hernandez, *Anal Chim Acta*, 242 (1991) 267
12. F. H. Keedy and P. Vadgama, *Biosens Bioelectron*, 6 (1991) 491
13. M.-J. Rocheleau and W. C. Purdy, *Electroanalysis*, 3 (1991) 935
14. A. K. Geim and K. S. Novoselov, *Nat Mater*, 6 (2007) 183
15. S. Alwarappan, A. Erdem, C. Liu and C.-Z. Li, *J Phys Chem*, 113 (2009) 8853
16. S. Guo, D. Wen, Y. Zhai, S. Dong and E. Wang, *ACS Nano*, 4 (2010) 3959
17. X. Kang, J. Wang, H. Wu, J. Liu, I. A. Aksay and Y. Lin, *Talanta*, 81 (2010) 754
18. F. Li, J. Chai, H. Yang, D. Han and L. Niu, *Talanta*, 81 (2010) 1063
19. M. Zhou, Y. Zhai and S. Dong, *Anal Chem*, 81 (2009) 5603
20. L. Fu, H. Liu, Y. Zou and B. Li, *Carbon*, 4 (2005) 10
21. W. S. Hummers and R. E. Offeman, *J Am Chem Soc*, 80 (1958) 1339
22. Y. Si and E. T. Samulski, *Nano Lett*, 8 (2008) 1679
23. L. Tang, Y. Wang, Y. Li, H. Feng, J. Lu and J. Li, *Adv Funct Mater*, 19 (2009) 2782
24. J.-S. Ye, Y. Wen, W. De Zhang, L. M. Gan, G. Q. Xu and F.-S. Sheu, *Electroanalysis*, 15 (2003) 1693
25. S. A. Kumar, H.-W. Cheng and S.-M. Chen, *Electroanalysis*, 21 (2009) 2281
26. W. Dong, J. Li and J. Guo, *Chem Res and Appl*, 20 (2008) 1235
27. S. Thiagarajan and S.-M. Chen, *Talanta*, 74 (2007) 212
28. J. Huang, Y. Liu, H. Hou and T. You, *Biosens Bioelectron*, 24 (2008) 632
29. C. Xiao, X. Chu, Y. Yang, X. Li, X. Zhang and J. Chen, *Biosens Bioelectron*, 26 (2011) 2934
30. M. Mallesha, R. Manjunatha, C. Nethravathi, G. S. Suresh, M. Rajamathi, J. S. Melo and T. V. Venkatesha, *Bioelectrochemistry*, 81 (2011) 104

31. J. Argüello, V. L. Leidens, H. A. Magosso, R. R. Ramos and Y. Gushikem, *Electrochim Acta*, 54 (2008) 560
32. R. Cui, X. Wang, G. Zhang and C. Wang, *"Sens Actuators, B "*, (2011)
33. L. Lin, J. Chen, H. Yao, Y. Chen, Y. Zheng and X. Lin, *Bioelectrochemistry*, 73 (2008) 11
34. R. P. da Silva, A. W. O. Lima and S. H. P. Serrano, *Anal Chim Acta*, 612 (2008) 89
35. Y. Li and X. Lin, *"Sens Actuators, B "*, 115 (2006) 134
36. P. Kalimuthu and S. A. John, *Talanta*, 80 (2010) 1686